

## New Software Simulating the Full Operation of a Scanning Tunneling Microscope and Its Application to an FPGA-Based Instrument

Mark J. Hagmann<sup>a</sup>, Gregory R. Spencer<sup>a</sup>, Jeremy Wiedemeier<sup>a</sup> and Marwan S. Mousa<sup>b</sup>

<sup>a</sup> *NewPath Research L.L.C., Salt Lake City, Utah 84115, USA.*

<sup>b</sup> *Department of Physics, Mu'tah University, Al-Karak 61710, Jordan.*

---

*Received on: 2/7/2018;*

*Accepted on: 22/10/2018*

---

**Abstract:** The scanning tunneling microscope is an essential tool in nanoscience and nanotechnology, because it enables imaging surfaces at the atomic level with sub-nanometer resolution. We have written a LabVIEW-based virtual instrument to simulate the operation of an STM and made it available as a free-download at our company website. This is an executable version to be run on a Windows operating system without requiring other software. We have also constructed an STM that implements the same algorithms with a field-programmable gate array (FPGA) to provide deterministic real-time control of multiple tasks.

**Keywords:** Scanning Tunneling Microscope, Field-Programmable Gate Array, Nanoscience, Nanotechnology.

### Introduction

The scanning tunneling microscope (STM), invented by Gerd Binnig and Heinrich Rohrer at IBM Zurich in 1986 [1], is an essential tool in nanoscience and nanotechnology. In an STM, a nanoscale metal tip electrode is brought within several tenths of a nanometer of an electrically-conductive sample and a DC bias voltage is applied to cause an electrical current to flow through this junction by quantum tunneling. Typically, a piezoelectric actuator is used to move the tip to adjust its distance from the sample as the tip is scanned to create images of the sample surface. The exponential sensitivity of the tunneling current to the tip-sample distance enables sub-nanometer resolution for images at the atomic level.

Others have written software to simulate the operation of an STM for classroom demonstrations [2] or created a simulator that may be downloaded for a trial period to demonstrate their products for imaging with an STM [3]. We have developed a LabVIEW

Virtual Instrument (VI) which simulates the full operation of an STM that may be downloaded from our company website for permanent use without registration, cost or time limits [4]. Documentation for the software and a narrated video showing typical operation of our simulator are also available at the website. The documentation includes figures, equations and definitions of the terminology. We hope that this VI will be useful for educational and training purposes. It was compiled using the LabVIEW Application Builder which allows stand alone applications to be bundled with the LabVIEW Run-Time Engine as an installer so the download does not require the installation of any other software. Our application was compiled to run on a Windows operating system, but if requested, we will modify the STM simulator VI so that it may be used on Mac operating systems as well. Fig. 1 shows the main display screen of the VI when imaging unreconstructed silicon (100).

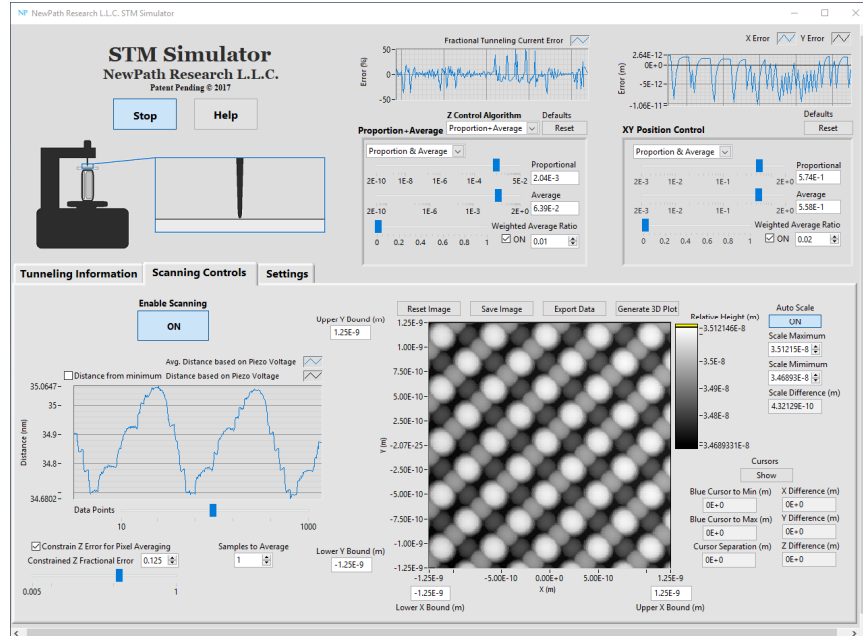


FIG. 1. Main display screen of the new STM simulator VI during operation, showing the unreconstructed surface of silicon (100). Image width = 2.5 nm.

## Materials and Methods

### Modeling of Non-Ideal Phenomena

To our knowledge, this is the first STM simulator to include the effects of noise in the tunneling current. Noise in the voltages controlling the x-, y- and z-motions of the piezoelectric actuator is modeled by introducing white Gaussian noise to the measured tunneling current. Stochastic slow-drift in the vertical position of the tip electrode which would be caused by vibration and temperature changes is modeled by gradually adjusting the tip-sample distance according to a random walk. The effects of the voltage drop on the series resistance, such as the spreading resistance in the sample at the tunneling junction, are also included. The adverse effects of blunted tips can be seen by adjusting the related parameters (such as the tip radius). We do not, however, model the effects of tips having unusual shapes such as double-pointed tips. Bounds for these non-ideal behaviors may be set by the user to determine their effects on measurements and imaging. We understand that other factors such as  $1/f$  noise, Johnson noise and generation-recombination noise may also have an effect on measurements [5]; however, these phenomena are yet included.

The software is written in a modular format to facilitate upgrading different parts to better

meet our needs and also to follow the suggestions from those who have downloaded this simulator VI. For example, we could model the resonances, nonlinearities and hysteresis in the response of the piezoelectric actuator which is used for fine-positioning of the tip electrode and may also provide different approximations to calculate the tunneling current including expressions for semiconductor samples.

### Four Methods for Feedback Control

Feedback control is used to adjust the tip-sample distance in an STM when initiating quantum tunneling and then to minimize the error in the tunneling current which is given by  $e(t) = I(t) - I_{SP}$ , where  $I(t)$  is the current at time  $t$  and  $I_{SP}$  is the chosen value for the set-point current. Simply making a change in the voltage  $\Delta V$  to the piezoelectric actuator that is proportional to the error is insufficient, because this would cause the tunneling current to oscillate about the set-point value.

PI (Proportion + Integral) feedback control, where the change in the voltage that is applied to the piezoelectric actuator is proportional to the sum of the error and the integral of the error, as shown in Eq. (1), is frequently used in scanning tunneling microscopy.

$$\Delta V = K_p e(t) + K_I \int_0^t e(t') dt' \quad (1)$$

Simulations made with the STM simulator VI show that PI feedback control is only stable over a specific range for the two coefficients  $K_p$  and  $K_I$  (see Fig. 2). The size and location of the stable region for these two coefficients depend on the properties of the tip and the tip-sample distance. Large oscillations in the tunneling

current, including the possibility of tip-crash failure or loss of tunneling, occur when one (or both) of these coefficients is outside the region for stability. It is inconvenient to have to estimate the value for both coefficients before the measurements.

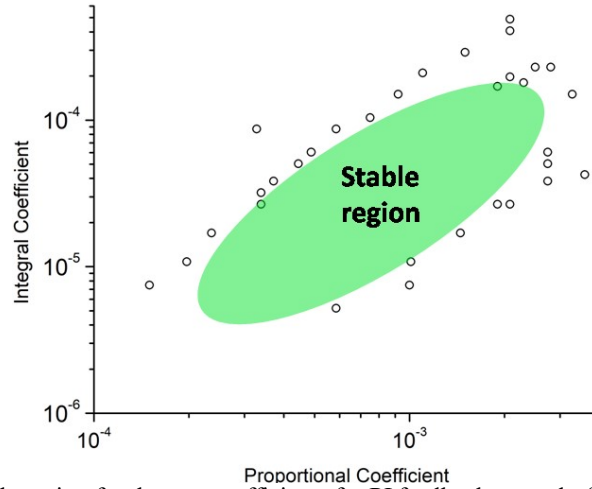


FIG. 2. Stable region for the two coefficients for PI feedback control of the tunneling current.

The control algorithms included in the VI are: (1) Unmodified PI as previously described, (2) D.A.S. (Digitally Adapted Steps) which adjusts the sizes of the steps of the piezoelectric actuator based on the tunneling current [6], (3) Modified Proportion in which the proportion coefficient is adjusted based on the tunneling current and (4) Proportion + Average which is similar to PI control but instead of integrating it takes the mean of the last few values of the error. Each of these algorithms is described in detail on our website.

The STM simulator VI may be used to compare the stability, response time and ease of use for feedback control of the current when using the four different algorithms with various values for their parameters.

### Stepper Motor and Piezoelectric Actuator

In order to obtain atomic resolution in imaging, the piezoelectric actuator must have a small range of motion (typically 60 nm). Thus, it is necessary to add a precision digital stepper motor for coarser positioning of the tip electrode in order to provide a greater range of motion in the system. The piezoelectric actuator is automatically decremented each time before the digital stepper motor is incremented to avoid missing specific tip-sample distances which

would be caused by the effects of the finite precision of the step motor.

### Simulation of Crystal Lattice Surfaces in Real-Time

Once the simulation shows that stable quantum tunneling has been achieved, it is possible to generate an image of highly ordered pyrolytic graphite (HOPG), graphene, unreconstructed silicon (100) or the reconstructed surface of silicon after it has been cleaved. The surfaces of these four materials were modeled by approximating the contours for the local density of states of electrons in the atoms as spheres with appropriate sizes. The images of the surfaces are created by scanning over the simulated surfaces while calculating the tunneling current based on the distance from the surface to the tip. Fig. 1 shows the main display screen when simulating the imaging of unreconstructed silicon (100). The graph at the lower left corner of this figure shows the relative height of the tip which is calculated from the voltage that is applied to the piezoelectric actuator. Oscillations in the height, which are seen in this graph, are caused by the tip electrode passing over several silicon atoms in the lattice.

At the upper left corner of Fig. 1, there is a sketch of the STM scan-head with an animated

diagram showing the vertical tip electrode above the horizontal sample. If the value calculated for the tip position is below the surface of the sample, indicating that a tip-crash has occurred, this cartoon shows that the tip is bent and the simulation has stopped. However, with an actual STM, it may not be obvious that a tip-crash has occurred, because images with high resolution are still possible. Thus, this feature enables the user to determine the optimum parameters to prevent tip-crash. Later, we will incorporate an algorithm to determine whether a tip-crash has occurred without relying on the simulated height of the tip. For example, a small increment in the voltage to the piezoelectric actuator would not change the current when the tip is in contact with the sample. This change would be necessary before the STM simulator VI software could be implemented in an actual STM.

In the constant current mode, feedback control of the tunneling current is enabled during scanning. In the constant height mode, feedback control is disabled during scanning so that the tip

is moved in a plane above the surface of the sample. This mode is prone to loss of tunneling or tip-crash unless it is used to image small areas or with samples having relatively flat surfaces.

## Results

Fig. 3 shows a graph of the simulated tunneling current over a specific time interval which is incremented throughout each session. This figure shows the effects of the noise in the tunneling current. A separate plot that is made over a much longer time interval is used to monitor the effects of feedback control on the tunneling current as well as the response to the simulated stochastic slow-drift.

After at least one line of a scan has been completed, a 3-D image of the sample may be generated as the data is collected for an image. Fig. 4 shows an example of a completed 3-D simulated image of unreconstructed silicon (100).

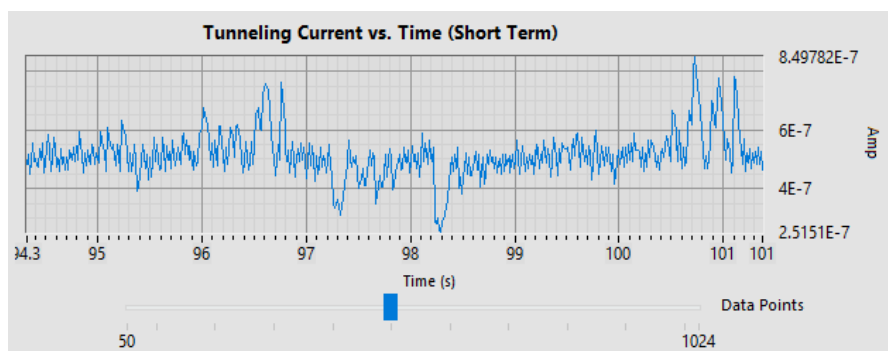


FIG. 3. Graph of the simulated tunneling current vs. time, showing the noise in the tunneling current.

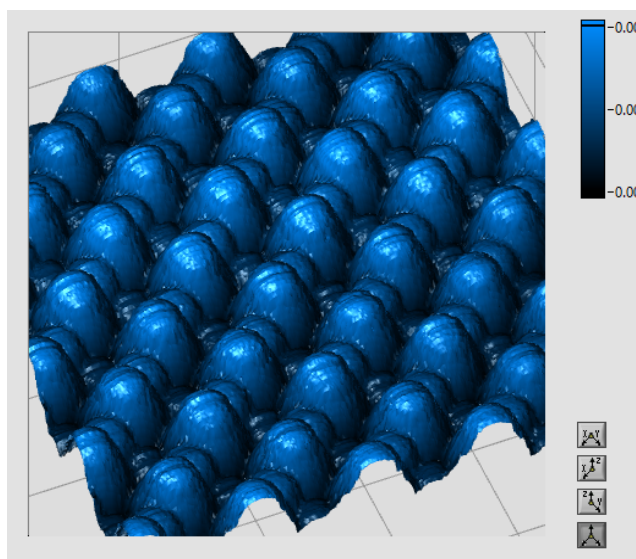


FIG. 4. Three-dimensional plot of a simulated image of unreconstructed silicon (100).

## Application of This Software to an FPGA-Based Instrument

Fig. 5 shows the scan-head of our portable in-house STM. This instrument has a reduced mechanical length for the C-shaped path between the tip and the sample with greater stiffness to provide unusually high stability. Thus, the tunneling typically continues automatically for a period of at least 72 hours. The software for the STM is written in

LabVIEW, input and output tools that are similar to those in the VI. There is also the same selection of algorithms for feedback control to increase the speed and accuracy of the measurements while reducing the probability of tip-crash. All of this is done using a field-programmable gate array (FPGA) to enable performing multiple deterministic tasks in real-time in addition to the feedback control of the tunneling current.

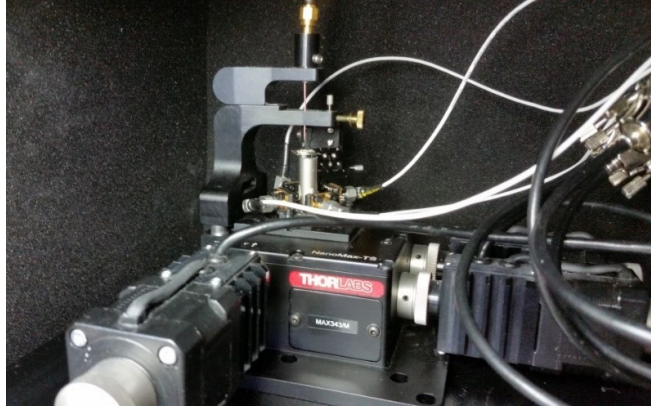


FIG. 5. Scan-head for our in-house STM.

This instrument was designed for experimental studies in which a microwave frequency comb is generated by focusing a mode-locked laser on the tunneling junction of an STM [7]. Thus, the tip electrode is attached to the center conductor of a semi-rigid coaxial cable to couple the microwave harmonics directly from the tunneling junction to a spectrum analyzer. A bias-T is attached to the SMA connector at the top end of this cable and its low-frequency port is connected to the low-noise STM preamplifier of the STM. The high-frequency port of the bias-T is connected to the spectrum analyzer or to an equivalent 50- $\Omega$  dummy load during calibration of the STM, in order to mitigate interference with the feedback control of the tunneling current.

## Conclusions

Our testing with this VI suggests that PID feedback control is effective after tunneling has been established. However, before there is a tunneling current, the history of zero current which is used as a criterion for the use of integration in feedback control delays the response when the current is first seen to potentiate the probability of tip-crash. Our results suggest that the method of D.A.S.

(Digitally Adapted Steps) simplifies the choice of the control parameters and provides fast response at the time when the tunneling current is first seen.

## Acknowledgment

This work is funded by the National Science Foundation under grant 164881.

## References

- [1] Binnig, G. and Rohrer, H., IBM J. Res. Dev., 30 (1986) 355.
- [2] Rebello, N.S. et al., Eur. J. Phys., 18 (1997) 456.
- [3] Specs Zurich GmbH, Zurich, [www.specs-zurich.com](http://www.specs-zurich.com).
- [4] NewPath Research L.L.C., Salt Lake City, Utah, [www.newpathresearch.com](http://www.newpathresearch.com).
- [5] Chen, C.J., "Introduction to Scanning Tunneling Microscopy", Oxford Series in Optical and Imaging Sciences, (1993), 252-253.
- [6] Hagmann, M.J., U.S. Patent 9, 885, 737 (2018).
- [7] Hagmann, M.J., Andrei, P., Pandey, S. and Nahata, A., J. Vac. Sci. Technol. B, 33(2015) 02B109.